Supplementary Materials

SUPPLEMENTARY METHODS

S1. Radiomics procedure

Image acquisition, segmentation and radiomics feature extraction

MRI images were downloaded from TCIA (http://www.cancerimagingarchive.net/). Contrast-enhanced weighted-T1 Digital Imaging and Communications in Medicine (DICOM) images were used for radiomics analysis. Those patients performed MRI examination before surgery were included in our study. Those have imaging artifacts in the MRI images were excluded. Finally, 47 ccRCC cases from the TCIA-KIRC project were used for radiomics analysis.

Volumes of interest (VOIs) of the tumor lesion were semi-automatically segmented using the *GrowCut* segmentation algorithms implemented in 3D Slicer software (version 4.9.0) [1,2]. VOI is initially delineated via the *GrowCut* segmentation method [2]. Then, radiologists meticulously edit the boundary of the regions of interest (ROIs) slice-by-slice manually, improving the alignment of the ROIs with the lesion outlines. All segmentations were performed by a radiologist with 8 years of experience and validated and revised by a senior radiologist with 19 years of experience.

In this study, 1316 candidate radiomics features were generated from images using the *PyRadiomics* platform implanted in Python software (version 3.7.4) [1]. As part of image preprocessing, images were resampled to isotropic voxels with 1-mm sides using a B Spline interpolator [3,4]. Target region intensity values were discretized using a bin width of 25. Aside from the original image, features were also extracted from wavelet and Laplacian of Gaussian (LoG)-filtered images.

The features were subdivided into five classes: first-order statistics features, shape- and size-based features, statistics-based textural features, features after wavelet transform, and LoG filtered features. Radiomics features in each class are described below and listed in Supplementary Table S1. More detailed descriptions of each feature are available in the *pyradiomics* documentation at http://pyradiomics.readthedocs.io/en/latest.

(1) First-order statistics features

First-order statistics describe the distribution of the voxel intensities within the image region defined by the mask through commonly used and basic metrics. A fuzzy similitude matrix, describing the image's feature space, is defined to analyze the spatial distribution of the pixels' hue matrix and extract static features of images. A total of 18 first-order statistics were used.

(2) Shape- and size-based features

This group of 14 features includes descriptors of the three-dimensional size and shape of the tumor lesion. They are only calculated on the non-derived image and mask because of independence from the gray-level intensity distribution in the ROI.

(3) Statistics-based textural features

Statistics-based textural features can reflect the homogeneity of the images and the arrangement of the properties that change slowly or periodically on the body surface. Five types of the matrix were included mainly in our textural features: (a) 24 gray-level co-occurrence matrix (GLCM) features; (b) 16 gray-level size zone matrix (GLSZM) features; (c) 16 gray-level run-length texture matrix (GLRLM) features; (d) 5 neighboring gray tone difference matrix (NGTDM) features, and (e) 14 gray level dependence matrix (GLDM) features.

A GLCM describes the distance and angle of each pixel, which calculates the correlation between two gray levels with certain directions and distances. A GLCM can reflect integrated information regarding the direction, interval, amplitude, and frequency of the images. A GLRLM quantifies gray-level runs, which are defined as the length in a number of pixels, of consecutive pixels that have the same gray-level value. Note that no weighting was applied in the calculation of the GLCM and GLRLM, and features were extracted for each of the 13 angles separately, representing the 26-connected region, after which the average value over all angles was returned as the extracted feature value. A GLSZM quantifies gray-level zones, that is, the number of connected voxels that share the same gray-level intensity. An NGTDM quantifies the difference between a gray value and the average gray value of its neighbors within a certain distance. The GLDM quantifies gray-level dependencies in an image, which is defined as the number of connected voxels within a certain distance that is dependent on the center voxel.

(4) Wavelet features

For the wavelet-filter, stationary wavelet transform was applied using the "coif1" (coiflet-1) wavelet function. The original image was decomposed in low- and high-frequencies using an undecimated three-dimensional wavelet transform, which can be considered as a preprocessing step before the extraction of features. Consider L and H to be low-pass and high-pass functions, respectively, X to be the decomposing image, and the wavelet decompositions of X to be labeled as $X_{LLL}, X_{LLH} X_{LHL}, X_{LHH}, X_{HLL}, X_{HLH}, X_{HHL}, X_{HHH}$, which represents eight new images in three directions (x, y, z). Wavelet decomposition focuses on the various frequency scales and different feature orientations

within brain lesion volume; nevertheless, the size of each decomposition is equal to the original image and each decomposition is shift-invariant. For each decomposition, the first-order statistical features and statistics-based textural features were computed as described above, resulting in 744 wavelet features.

(5) LoG filtered features

The original images were filtered using a 3D LoG filter implemented in SimpleITK and by changing sigma values to 5.0, 4.0, 3.0, 2.0 and 1.0 mm, yielding another 5 derived images. For each filtering, the first-order statistical features and statistics-based textural features were computed as described above, resulting in 465 wavelet features.

S2. Detailed description of the LASSO method

LASSO is a powerful method for regression with high dimensional predictors. In our study, the LASSO method was combined with logistic regression model for analysis of the m6A subtype, which could select the most important predictive features from the training set. This method minimizes a log partial likelihood subject to the sum of the absolute values of the parameters being bounded by a constant:

$$\hat{\beta} = \text{argmin } \ell(\beta), \text{ subject to } \sum|\beta_j| \leq s$$

where, $\hat{\beta}$ is the obtained parameters, $\ell(\beta)$ is the log partial likelihood of the logistic regression model, $s > 0$ is a constant.

The LASSO method can be used for feature reduction and selection by shrinking coefficients and forcing certain coefficients to be set to zero through absolute constraint. In this study, the standardized constraint parameter s was set as 0.096 and 7 nonzero coefficients ($\hat{\beta}$) were selected by LASSO.

S3. R packages used in this Study

All statistical analyses were performed using R statistical software version 4.0.4 (https://www.r-project.org/). R packages used in this study are listed as follows:

Statistical analysis	R package
Differential expression analyses	limma
Heatmap	pheatmap
Correlation plot	corrplot
LASSO cox regression analyses	glmnet
ROC curves	pROC
Kaplan-Meier curve	Survival survminer
Forest plot	forestplot

REFERENCES

1. van Griethuysen JJM, Fedorov A, Parmar C, et al. Computational Radiomics System to Decode the Radiographic Phenotype. *Cancer research.* 2017;77(21):e104-e107.

2. Egger J, Kapur T, Dukatz T, et al. Square-cut: a segmentation algorithm on the basis of a rectangle shape. *PloS one.* 2012;7(2):e31064.

3. van Griethuysen JJM, Fedorov A, Parmar C, et al. Computational radiomics system to decode the radiographic phenotype. *Cancer research.* 2017;77(21):e104–e107.

4. Sun R, Limkin EJ, Vakalopoulou M, et al. A radiomics approach to assess tumour-infiltrating CD8 cells and response to anti-PD-1 or anti-PD-L1 immunotherapy: an imaging biomarker, retrospective multicohort study. *The Lancet Oncology.* 2018;19(9):1180–1191.

5. Landis JR, Koch GG. The measurement of observer agreement for categorical data. *Biometrics.* 1977;33(1):159-174.

SUPPLEMENTARY TABLES

Table S1. Extracted radiomics features.

Group	Subgroup	Radiomics Features
First-order statistics features		Interquartile Range, Skewness, Uniformity, Median, Energy, Robust Mean Absolute Deviation, Mean Absolute Deviation, Total Energy, Maximum, Root Mean Squared, 90th Percentile, Minimum, Entropy, Range, Variance, 10th Percentile, Kurtosis, Mean
Shape-based features		Voxel Volume, Mesh Volume, Surface Volume Ratio, Maximum 3D Diameter, Maximum 2D Diameter Slice, Sphericity, Minor Axis, Elongation, Major Axis, Surface Area, Flatness, Least Axis, Maximum 2D Diameter Column, Maximum 2D Diameter Row
Statistics-based textural features	**GLCM**	Joint Average, Sum Average, Joint Entropy, Cluster Shade, Maximum Probability, Inverse Difference Moment Normalized, Joint Energy, Contrast, Difference Entropy, Inverse Variance, Difference Variance, Inverse Difference Normalized, Inverse Difference Moment, Correlation, Autocorrelation, Sum Entropy, Maximal Correlation Coefficient, Sum Squares, Cluster Prominence, Informal Measure of Correlation 2, Informal Measure of Correlation 1, Difference Average, Inverse Difference, Cluster Tendency
	GLRLM	Short Run Low Gray Level Emphasis, Gray Level Variance, Low Gray Level Run Emphasis, Gray Level Non-Uniformity Normalized, Run Variance, Gray Level Non-Uniformity, Long Run Emphasis, Short Run High Gray Level Emphasis, Run Length Non-Uniformity, Short Run Emphasis, Long Run High Gray Level Emphasis, Run Percentage, Long Run Low Gray Level Emphasis, Run Entropy, High Gray Level Run Emphasis, Run Length Non-Uniformity Normalized
	GLSZM	Gray Level Variance, Zone Variance, Gray Level Non-Uniformity Normalized, Size Zone Non-Uniformity Normalized, Size Zone Non-Uniformity, Gray Level Non-Uniformity, Large Area Emphasis, Small Area High Gray Level Emphasis, Zone Percentage, Large Area Low Gray Level Emphasis, Large Area High Gray Level Emphasis, High Gray Level Zone Emphasis, Small Area Emphasis, Low Gray Level Zone Emphasis, Zone Entropy, Small Area Low Gray Level Emphasis
	GLDM	Gray Level Variance, High Gray Level Emphasis, Dependence Entropy, Dependence Non-Uniformity, Gray Level Non-Uniformity, Small Dependence Emphasis, Small Dependence High Gray Level Emphasis, Dependence Non-Uniformity Normalized, Large Dependence Emphasis, Large Dependence Low Gray Level Emphasis, Dependence Variance, Large Dependence High Gray Level Emphasis, Small Dependence Low Gray Level Emphasis, Low Gray Level Emphasis
	NGTDM	Coarseness, Complexity, Strength, Contrast, Business
Wavelet features[*]		wavelet(LLL)_x, wavelet(LLH)_x, wavelet(LHL)_x, wavelet(LHH)_x, wavelet(HLL)_x, wavelet(HLH)_x, wavelet(HHL)_x, wavelet(HHH)_x
LoG filtered features[*]		LoG(σ=1)_x, LoG(σ=2)_x, LoG(σ=3)_x, LoG(σ=4)_x, LoG(σ=5)_x

[*]x denotes the first-order statistics features and statistics-based textural features listed above.

Abbreviations: LoG: Laplacian of Gaussian; GLSZM: Gray Level Size Zone Matrix; GLRLM: Gray Level Run Length Matrix; GLDM: Gray Level Dependence Matrix; GLCM: Gray Level Cooccurence Matrix; NGTDM, neighboring gray tone difference matrix.

Table S2. Baseline characteristics of the patients in the training and validation sets.

Characteristic	Training set (n = 371)	Validation set (n = 159)	*P*
Age, years			
Median (Interquartile range)	60 (51, 69)	61 (53, 71)	0.505
Sex			0.780
Female	130 (35.0)	53 (33.3)	
Male	241 (65.0)	106 (66.7)	
Tumor grade			0.384
G1	11 (3.0)	2 (1.3)	
G2	154 (41.5)	76 (47.8)	
G3	144 (38.8)	61 (38.4)	
G4	55 (14.8)	19 (11.9)	
Gx	7 (1.9)	1 (0.6)	
T stage			0.466
T1	184 (49.6)	86 (54.1)	
T2	51 (13.7)	19 (11.9)	
T3	130 (35.0)	49 (30.8)	
T4	6 (1.6)	5 (3.1)	
N stage			0.420
N0	162 (43.7)	77 (48.4)	
N1	13 (3.5)	3 (1.9)	
Nx	196 (52.8)	79 (49.7)	
M stage			0.246
M0	288 (77.6)	134 (84.3)	
M1	59 (15.9)	19 (11.9)	
Mx	24 (6.5)	6 (3.8)	
Neoadjuvant treatment			1.000
No	359 (96.8)	154 (96.9)	
Yes	12 (3.2)	5 (3.1)	
Survival status			0.871
Alive	250 (67.4)	109 (68.6)	
Dead	121 (32.6)	50 (31.4)	

Data are presented as No. (%) unless indicated otherwise.

P values were derived from the univariate association analyses between the training and validation set.

Table S3. Potential predictors of overall survival in patients with ccRCC.

Variables	Univariate Cox regression		Multivariate Cox regression	
	HR (95% CI)	*P*	HR (95% CI)	*P*
Age	1.029 (1.016-1.043)	<0.001*	1.027 (1.013-1.041)	<0.001*
Sex (male *vs.* female)	0.945 (0.690-1.294)	0.724	-	-
Tumor grade (G1-2 *vs.* G3-4)	2.716 (1.921-3.841)	<0.001*	1.805 (1.255-2.597)	0.001*
T stage (T1-2 *vs.* T3-4)	3.131 (2.302-4.260)	<0.001*	-	-
N stage				
N0	Reference		Reference	
N1	3.224 (1.668-6.230)	<0.001*	1.517 (0.767-3.002)	0.231
Nx	0.813 (0.596-1.110)	0.194	0.703 (0.512-0.966)	0.030
M stage				
M0	Reference		Reference	
M1	4.343 (3.167-5.954)	<0.001*	2.672 (1.884-3.789)	<0.001*
Mx	0.975 (0.308-3.082)	0.965	0.627 (0.197-1.997)	0.430
Neoadjuvant treatment (no *vs.* yes)	2.150 (1.134-4.076)	0.019*	-	-
m6A subtype (low *vs.* high score)	4.057 (2.986-5.511)	<0.001*	2.795 (1.999-3.907)	<0.001*

Abbreviations: ccRCC: clear cell renal cell carcinoma; HR, hazard ratio; CI, confidence interval.

Table S4. Model comparisons using C-index in all enrolled patients.

Models	C-index (95% CI)
m6A subtype	0.698 (0.657-0.739)
Age	0.592 (0.547-0.637)
Sex	0.508 (0.469-0.547)
Tumor grade	0.628 (0.593-0.663)
T stage	0.663 (0.626-0.700)
N stage	0.555 (0.513-0.597)
M stage	0.647 (0.609-0.685)
Neoadjuvant treatment	0.513 (0.496-0.530)
Age + Tumor grade + T stage + N stage	0.753 (0.714-0.792)
m6A subtype+ Age + Tumor grade + T stage + N stage	0.786 (0.752-0.820)

Abbreviation: CI, confidence interval.

SUPPLEMENTARY FIGURES

Figure S1. Correlation between the selected m6A regulators and prognosis in ccRCC patients.

Kaplan-Meier survival curves of patients with low or high expressions of the five selected prognosis-related m6A regulators in all patients.

Abbreviation: ccRCC: clear cell renal cell carcinoma; CI, confidence interval.
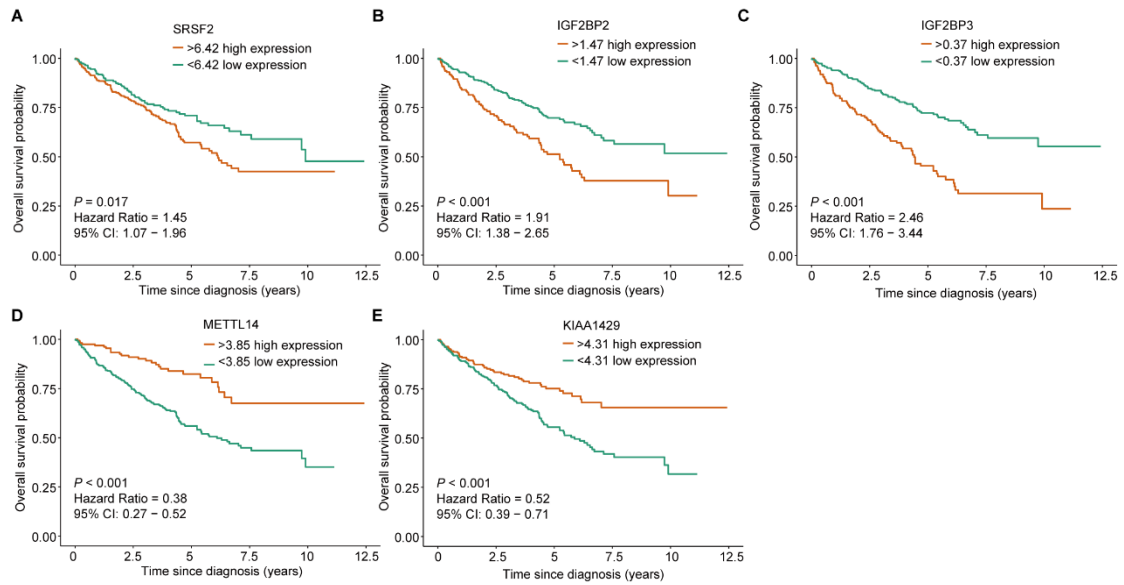
Figure S2. X-tile plots identifying the optimal cutoff m6A score based on overall survival.

(A) X-tile plot for the training set. The coloration of the plot represents the strength of the association at each division, ranging from low (dark, black) to high (bright, green). (B) The distribution of the number of patients by m6A score.

(C) A Kaplan-Meier plot categorized by the low and high m6A score groups according to the optimal cutoff value. The optimal cutoff value of the m6A score was determined as 1.10 based on overall survival (χ^2 = 71.368, P <0.0001).
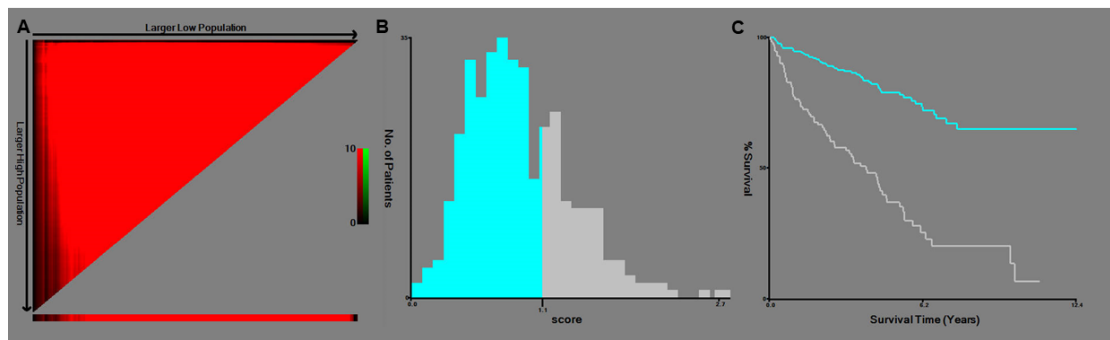
Figure S3. The genetic mutation landscape for ccRCC in different m6A subtypes.

Waterfall plot displaying the landscapes of frequently mutated genes in all eligible ccRCC patients (A), patients with high m6A scores (B), and patients with low m6A scores (C). Genes are ordered according to their mutation frequency, and different mutation types were presented as indicated by the annotation bar.